

MIT Open Access Articles

*Multiband plasmonic absorber based
on transverse phase resonances*

The MIT Faculty has made this article openly available. **Please share**
how this access benefits you. Your story matters.

Citation: Cui, Yanxia et al. "Multiband Plasmonic Absorber Based on Transverse Phase Resonances." *Optics Express* 20.16 (2012): 17552. © 2012 OSA

As Published: <http://dx.doi.org/10.1364/OE.20.017552>

Publisher: Optical Society of America

Persistent URL: <http://hdl.handle.net/1721.1/78306>

Version: Final published version: final published article, as it appeared in a journal, conference proceedings, or other formally published context

Terms of Use: Article is made available in accordance with the publisher's policy and may be subject to US copyright law. Please refer to the publisher's site for terms of use.



Multiband plasmonic absorber based on transverse phase resonances

Yanxia Cui,^{1,2,3,*} Kin Hung Fung,^{2,4} Jun Xu,^{2,4} Sailing He,³ and Nicholas X. Fang^{2,4,5}

¹College of Physics and Optoelectronics, Taiyuan University of Technology, Taiyuan 030024, China

²University of Illinois at Urbana-Champaign, Urbana, Illinois 61801, USA

³Centre for Optical and Electromagnetic Research, State Key Laboratory of Modern Optical Instrumentation, JORCEP (KTH-ZJU Joint Center of Photonics), Zhejiang University, Hangzhou, Zhejiang 310058, China

⁴Department of Mechanical, Massachusetts Institute of Technology, Cambridge, Massachusetts 02139, USA

⁵nicfang@mit.edu
*yanxiacui@gmail.com

Abstract: We demonstrate a multiband plasmonic absorber based on transverse phase resonances. We show that the modification of conventional metallic surfaces of T-shape grooves can cause mode splitting of the plasmonic waveguide cavity modes due to lattice scattering and all the new resonant modes exhibit large absorptivity greater than 90%. Some of the generated absorption peaks have wide-angle characteristics. Furthermore, we find that the proposed structure is fairly insensitive to the alignment error between different layers.

©2012 Optical Society of America

OCIS codes: (240.6680) Surface plasmons; (310.3915) Metallic, opaque, and absorbing coatings; (260.5740) Resonance.

References and links

1. R. W. Wood, "On a remarkable case of uneven distribution of light in a diffraction grating spectrum," Proc. Phys. Soc. Lond. **18**(1), 269–275 (1901).
2. S. A. Maier, *Plasmonics: fundamentals and applications* (Springer, 2007).
3. T. López-Rios, D. Mendoza, F. J. Garcia-Vidal, J. Sanchez-Dehesa, and B. Pannetier, "Surface shape resonances in lamellar metallic gratings," Phys. Rev. Lett. **81**(3), 665–668 (1998).
4. N. Bonod, G. Tayeb, D. Maystre, S. Enoch, and E. Popov, "Total absorption of light by lamellar metallic gratings," Opt. Express **16**(20), 15431–15438 (2008).
5. N. I. Landy, S. Sajuyigbe, J. J. Mock, D. R. Smith, and W. J. Padilla, "Perfect metamaterial absorber," Phys. Rev. Lett. **100**(20), 207402 (2008).
6. E. Popov, S. Enoch, and N. Bonod, "Absorption of light by extremely shallow metallic gratings: metamaterial behavior," Opt. Express **17**(8), 6770–6781 (2009).
7. T. V. Teperik, F. J. Garcia de Abajo, A. G. Borisov, M. Abdelsalam, P. N. Bartlett, Y. Sugawara, and J. J. Baumberg, "Omnidirectional absorption in nanostructured metal surfaces," Nat. Photonics **2**(5), 299–301 (2008).
8. J. Hao, J. Wang, X. Liu, W. J. Padilla, L. Zhou, and M. Qiu, "High performance optical absorber based on a plasmonic metamaterial," Appl. Phys. Lett. **96**(25), 251104 (2010).
9. H. A. Atwater and A. Polman, "Plasmonics for improved photovoltaic devices," Nat. Mater. **9**(3), 205–213 (2010).
10. C. Wu, B. Neuner III, J. John, A. Milder, B. Zollars, S. Savoy, and G. Shvets, "Metamaterial-based integrated plasmonic absorber/emitter for solar thermo-photovoltaic systems," J. Opt. **14**(2), 024005 (2012).
11. N. Liu, M. Mesch, T. Weiss, M. Hentschel, and H. Giessen, "Infrared perfect absorber and its application as plasmonic sensor," Nano Lett. **10**(7), 2342–2348 (2010).
12. W. S. Chang, J. W. Ha, L. S. Slaughter, and S. Link, "Plasmonic nanorod absorbers as orientation sensors," Proc. Natl. Acad. Sci. U.S.A. **107**(7), 2781–2786 (2010).
13. M. J. Lockyear, A. P. Hibbins, J. R. Sambles, P. A. Hobson, and C. R. Lawrence, "Thin resonant structures for angle and polarization independent microwave absorption," Appl. Phys. Lett. **94**(4), 041913 (2009).
14. H. Tao, C. Bingham, A. Strikwerda, D. Pilon, D. Shrekenhamer, N. Landy, K. Fan, X. Zhang, W. Padilla, and R. Averitt, "Highly flexible wide angle of incidence terahertz metamaterial absorber: Design, fabrication, and characterization," Phys. Rev. B **78**(24), 241103 (2008).
15. Y. Q. Ye, Y. Jin, and S. He, "Omnidirectional, polarization-insensitive and broadband thin absorber in the terahertz regime," J. Opt. Soc. Am. B **27**(3), 498–504 (2010).
16. Z. H. Jiang, S. Yun, F. Toor, D. H. Werner, and T. S. Mayer, "Conformal dual-band near-perfectly absorbing mid-infrared metamaterial coating," ACS Nano **5**(6), 4641–4647 (2011).
17. Y. Cui, J. Xu, K. Hung Fung, Y. Jin, A. Kumar, S. He, and N. X. Fang, "A thin film broadband absorber based on multi-sized nanoantennas," Appl. Phys. Lett. **99**(25), 253101 (2011).

18. C. Wu and G. Shvets, "Design of metamaterial surfaces with broadband absorbance," *Opt. Lett.* **37**(3), 308–310 (2012).
19. C. W. Cheng, M. N. Abbas, C. W. Chiu, K. T. Lai, M. H. Shih, and Y.-C. Chang, "Wide-angle polarization independent infrared broadband absorbers based on metallic multi-sized disk arrays," *Opt. Express* **20**(9), 10376–10381 (2012).
20. J. Hendrickson, J. Guo, B. Zhang, W. Buchwald, and R. Soref, "Wideband perfect light absorber at midwave infrared using multiplexed metal structures," *Opt. Lett.* **37**(3), 371–373 (2012).
21. J. Yang, X. Hu, X. Li, Z. Liu, Z. Liang, X. Jiang, and J. Zi, "Broadband absorption enhancement in anisotropic metamaterials by mirror reflections," *Phys. Rev. B* **80**(12), 125103 (2009).
22. J. Sun, L. Liu, G. Dong, and J. Zhou, "An extremely broad band metamaterial absorber based on destructive interference," *Opt. Express* **19**(22), 21155–21162 (2011).
23. Y. Cui, K. H. Fung, J. Xu, H. Ma, Y. Jin, S. He, and N. X. Fang, "Ultrabroadband light absorption by a sawtooth anisotropic metamaterial slab," *Nano Lett.* **12**(3), 1443–1447 (2012).
24. E. Moreno, F. J. Garcia-Vidal, S. G. Rodrigo, L. Martin-Moreno, and S. I. Bozhevolnyi, "Channel plasmon-polaritons: modal shape, dispersion, and losses," *Opt. Lett.* **31**(23), 3447–3449 (2006).
25. T. Søndergaard and S. Bozhevolnyi, "Surface-plasmon polariton resonances in triangular-groove metal gratings," *Phys. Rev. B* **80**(19), 195407 (2009).
26. A. P. Hibbins, I. R. Hooper, M. J. Lockyear, and J. R. Sambles, "Microwave transmission of a compound metal grating," *Phys. Rev. Lett.* **96**(25), 257402 (2006).
27. M. Navarro-Cía, D. C. Skigin, M. Beruete, and M. Sorolla, "Experimental demonstration of phase resonances in metallic compound gratings with subwavelength slits in the millimeter wave regime," *Appl. Phys. Lett.* **94**(9), 091107 (2009).
28. E. D. Palik, *Handbook of Optical Constants of Solids* (Academic Press, 1998).
29. M. G. Moharam and T. K. Gaylord, "Rigorous coupled-wave analysis of metallic surface-relief gratings," *J. Opt. Soc. Am. A* **3**(11), 1780–1787 (1986).
30. Y. Xie, A. Zakharian, J. Moloney, and M. Mansuripur, "Transmission of light through slit apertures in metallic films," *Opt. Express* **12**(25), 6106–6121 (2004).

1. Introduction

While a flat metallic surface strongly reflects light rather than absorbs light, we could obtain anomalous strong light absorption by structuring the metal surface [1]. The anomalous light absorption in metal structures is mainly due to excitation of surface plasmon polaritons (SPPs) or localized surface plasmon polaritons (LSPPs) [2]. Recently, lots of different kinds of perfect absorbers based on SPPs or LSPPs (i.e., plasmonic absorbers) [3–8] have emerged, opening many opportunities for applications in thin film solar cells [9], thermal photovoltaics and thermal emitters [10], and highly sensitive bio-sensors [11,12]. Besides, perfect electromagnetic energy absorptions in structured metal surfaces have also been demonstrated in the gigahertz [13] and terahertz regimes [14].

The past research reflects that it is not hard to construct plasmonic absorbers at single resonant band. It is, however, desirable to have perfect absorptions over broad spectral bands (or at least over multi-bands) in order to collect as more incident energy as possible. Many approaches such as combining different resonators [15–20], forming anti-reflection effects [21,22], and exciting slow-light waves [23] have been used to achieve broadband or multiband absorption. In this paper, we propose an alternative method to broaden the absorption band of absorbers based on traditional plasmonic waveguides. The earliest absorbers based on plasmonic waveguides are of rectangular cross section [3,4], but they have relatively inferior performances on localizing and guiding light compared to the V-groove waveguides of triangular-shaped cross-sections [24,25]. By modifying the V-groove structure and introducing some additional phase resonances [26,27] along the horizontal axis, we show that a moderate absorption peak could be split into two distinct peaks of enhanced absorption due to lattice scattering.

2. Structures and methods

We compare two kinds of two-dimensional (2D) metallic structures as shown in Fig. 1. The periodic T-shape groove structure in Fig. 1(a) is a modified structure of the original V-groove structure used in Ref [25]. The array of T-shape grooves has a spatial period, P , and each groove is composed of a wide groove (of width W_1 and height h_1) over a narrow groove (of width W_2 and height h_2). The other structure in Fig. 1(b) is our proposed structure, which is formed by cutting the metal horizontally at the bottleneck of the T-groove in Fig. 1(b) and

drilling three additional narrow grooves. Such a structure has a narrow horizontal gap of d . The additional narrow grooves are identical to the bottom part of the original T-groove and all the narrow grooves are equally separated. For simplicity, we consider all gaps and grooves are filled with air in our simulations, while in practice air should be replaced by some dielectrics and the geometrical parameters need to be tuned accordingly for maximum absorption.

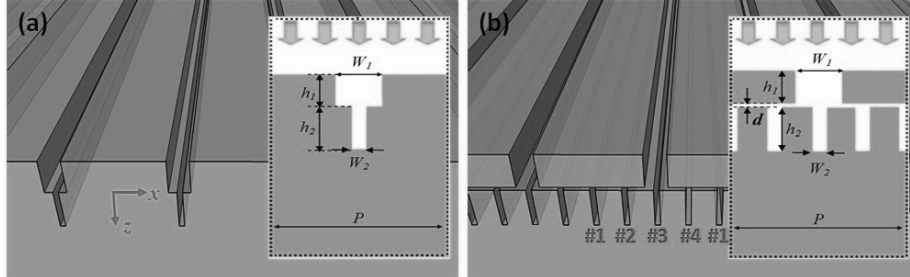


Fig. 1. Sketches of the original T-groove metallic surface (a) and the proposed light absorber (b). Insets are the cross sections in the x - z plane. Within a period, the grooves are labeled from #1 to #4 and the next period starts with label #1.

The present design works only for an incident plane wave of TM polarization (with magnetic field H_y perpendicular to the x - z plane) and it may not be directly generalized to absorb both polarizations. The metal is considered to be silver in our simulation and its permittivity parameters are obtained from Ref [28]. The bottom metal layer is assumed to be thick enough so that there is no light transmission ($T = 0$). Rigorous Coupled-wave Analysis (RCWA) method [29], which has been verified by studying the structures in Ref [30], is employed in the simulation. The absorptivity (η) is then calculated from the reflectivity (R) including all reflections orders by the formula $\eta = 1-R$. Unless otherwise mentioned, the geometrical parameters we use are $P = 1,100$ nm, $W_1 = 200$ nm, $h_1 = 300$ nm, $W_2 = 50$ nm, $h_2 = 350$ nm, and $d = 30$ nm.

3. Results and discussions

The calculated normal-incidence absorption spectra as a function of photon energies ($\hbar\omega$) are plotted in Fig. 2(a). It is obvious that the modified metallic structure (solid) absorbs light much better than the original design (dashed). We have also calculated the integrated absorption efficiency (β) within the range of [0.3, 1] eV for the two absorbers. Results shows that β equals to 32.6% for our multiband absorber, which is around 50% greater than that of the original T-groove case ($\beta = 22.2\%$). We note that for the original T-groove structure, its absorption spectra can be optimized by tuning the periodicity (P) [25] and the optimized value of the integrated absorption efficiency is around 22.8%, much lower than that of our multiband absorber as well.

To explain the detailed physical mechanism, we begin with a brief study of the original T-groove metallic surface. In Fig. 2(a), it is shown that this T-groove metallic surface could absorb light with an efficiency of about 65% at two frequencies (i.e., $\hbar\omega = 0.42$ and 0.81 eV). This absorbing effect should be attributed to the plasmonic waveguide cavity modes related to the geometry of individual grooves [3,4,25]. At the first absorption peak ($\hbar\omega_{01}$), each T-groove supports the first order Fabry-Perot (F-P) resonance of π length phase with the groove height causing light propagation to experience a phase shift of $\pi/2$ and the bottom surface of the metallic groove giving an additional $\pi/2$ phase shift by mirror reflection, which can be seen clearly from the distributions of field magnitude $|H_y|$ and phase $\Phi(H_y)$ in Fig. 3(a). At the second peak ($\hbar\omega_{02}$), a higher order F-P resonance arises with one field node along the vertical direction [Fig. 3(d)] thus each groove works as a cavity of 3π phase length considering the mirror effect by the bottom surface of metallic groove. In the left panel of

Fig. 2(b), we plot the band diagram [i.e., the angular spectrum as a function of photon energies and the horizontal component of incident wave vector (K_x)] of this T-groove surface. It is seen that the first order resonance (around 0.42 eV) has a very wide solid angle of absorption (with θ about 70°). This nearly angle-independent resonance is common for plasmonic waveguide cavity modes. However, when the neighboring resonant cavities are coupled and interact with free photons, there is a strong dependence of the photon energy on the angle of incidence and the band becomes dispersive. This is the case for the second order resonance at about 0.81 eV. It should be noted that there is a band-folding effect in our band diagram because the period of our structure ($P = 1,100$ nm) is comparable to the corresponding wavelength of free photons at $\hbar\omega_2$ ($\lambda = 1,530$ nm). To show the coupling between free photons and the surface plasmons, we also plot the folded light-line (thick white solid) in Fig. 2(b). It is clear that, unlike the first order resonance, the second order resonance is disturbed by free photons so that the solid angle of absorption at $\hbar\omega_2$ is less than 15° .

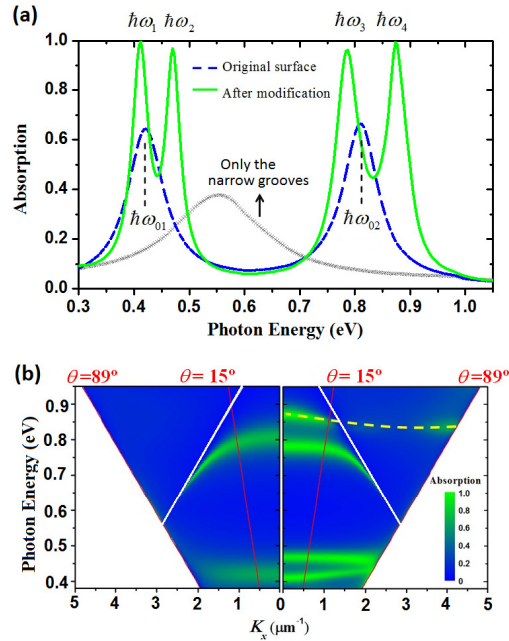


Fig. 2. (a) Absorption spectra as a function of photon energies for the original T-groove surface (dashed line) and our proposed structure (solid line). All of their absorption peaks are labeled. The absorption spectra for the metallic surface with only the bottom narrow grooves is also displayed by the cross line. (b) The band diagram for the original T-groove surface (left panel) and our proposed structure (right panel) with the thick white solid line representing the folded light line. Thin red solid lines indicate the light line for $\theta = 15^\circ$ and 89° . The dashed line in the right panel of (b) indicates the trend of the band of ω_4 .

In contrast, the absorption spectrum for our proposed structure [solid curve, Fig. 2(a)] exhibits four strong absorption peaks located at $\hbar\omega = 0.41, 0.47, 0.79,$ and 0.87 eV, labeled as $\omega_1, \omega_2, \omega_3,$ and ω_4 , respectively. All these four peaks have much higher theoretical absorption efficiencies $\eta > 96\%$, and they can be grouped into two types. The two peaks at ω_1 and ω_2 belong to the first type, which is associated with the first order mode (ω_{01}) of the original T-groove, while the other two peaks at ω_3 and ω_4 belong to the second type, which is associated with the second order mode (ω_{02}). The band diagram of our modified structure is also shown in the right panel of Fig. 2(b) in contrast with that of the original T-groove surface. One sees that the two resonances of the first type (ω_1 and ω_2) are almost angle independent (θ could approach 89°), while the other two resonances of the second type (ω_3

and ω_4) are influenced a lot by the free-photon dispersion; this is exactly in accordance with the resonances at ω_{01} and ω_{02} for the original T-groove surface. It should be noted that the band at ω_4 [dashed line, Fig. 2(b)] is relatively flat as compared to the band at ω_3 . And this will be explained later.

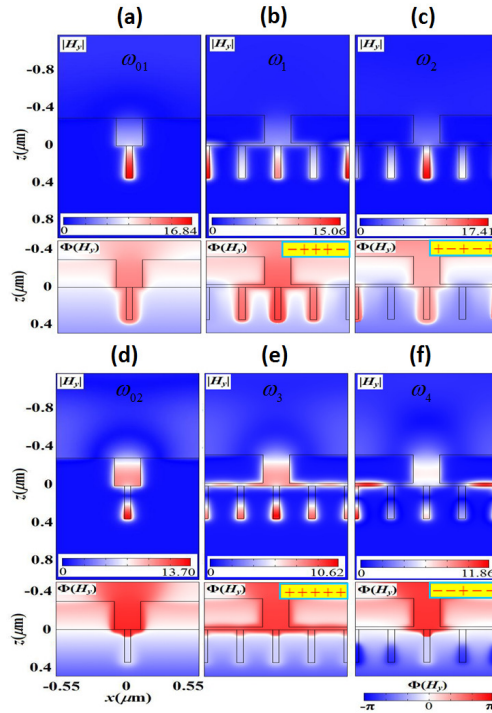


Fig. 3. (a-f) Distributions of magnetic field $|H_y|$ and phase $\Phi(H_y)$ for the absorption peaks of ω_{01} , ω_1 , ω_2 , ω_{02} , ω_3 , and ω_4 , as labeled in Fig. 2(a). Insets of $\Phi(H_y)$ in (b-c) and (e-f) show the phase states of each resonance near the opening of the bottom narrow grooves. Signs ‘+’ and ‘-’ represent a phase close to π and 0, respectively.

In order to understand the four plasmon modes of our proposed structure, we have also studied the distributions of field magnitude $|H_y|$ and phase $\Phi(H_y)$ [see Fig. 3(b), 3(c), 3(e), and 3(f)]. It should be noted that the absorption properties show a strong dependence on the total number of grooves N in one period (discussed at the end of this section). In Fig. 1(b), we have four narrow grooves in each period (i.e., $N = 4$). We label the grooves within a period from #1 to #4 as shown in Fig. 1(b) (groove #1 is separated into two halves in our defined unit cell). If we only consider the field distribution within the middle groove (#3) and also the top part of the T-grooves, we see that both the magnitude and phase distributions of the first type [Fig. 3(b) and 3(c)] is very close to that of the original case [Fig. 3(a)]. This is also true for the second type [Fig. 3(e) and 3(f)] versus the original case [Fig. 3(d)]. It means that, for our proposed metallic structure, although a horizontal gap geometrically breaks the original T-groove into two parts, this gap of value $d = 30$ nm is too small to alter the field distribution within the T-groove.

Since there are additional narrow grooves that can support resonances, part of the field energy is coupled to the modes in these narrow grooves after we open the horizontal air gap. For instance, as shown in Fig. 3(b), groove #1 can have a concentrated field that is even higher than groove #3 for the peak at ω_1 . Such phenomenon also occurs for the peak at ω_4 [Fig. 3(f)]. This might be the reason for the relatively flat band at resonance ω_4 in comparison with that at ω_3 as we mentioned earlier on Fig. 2(b). At ω_4 , attributed to the higher energy

concentration within the region of groove #1, which does not directly interact with the incident light, the whole coupling to free photons are relatively weaker and less sensitive to dispersion. However, at ω_3 , the electromagnetic field in the T-groove part is comparably stronger than that in other narrow grooves. This feature indicates that the whole structure would strongly interact with the incident free photon, which causes a dispersive absorption band just as that at ω_{b2} for the original T-groove surface.

The additional narrow grooves, opened in the bottom layer, play a significant role of boosting absorption and overcoming the narrow bandwidth of traditional absorbers. Such pronounced effect is due to the π phase change generated by these openings along the horizontal direction. In Fig. 3(b) and 3(c), we see that although the resonances at ω_1 and ω_2 are of the same type, they are different in terms of the phase information along x -direction. If we consider the phase near the opening of each groove, the phase distribution at ω_1 and ω_2 can be represented by ‘- + + -’ and ‘+ - - +’, respectively (the sequence of signs corresponds to the field sign at the opening of grooves #1, #2, #3, #4, and the next #1 at a certain time). Here, similar to a previous work [26], we use the sign ‘+’ to represent a phase close to π and the sign ‘-’ to represent a phase close to zero. At ω_1 and ω_2 , we find that there is a phase change of π and 2π , respectively, within one period along the x axis. Such phase information suggests that the resonance at ω_1 and ω_2 can be considered as a surface plasmon resonance with a wavenumber (or momentum) of $2\pi/P$ and $4\pi/P$, respectively. The excitation of finite parallel momentum at normal incidence is due to the lattice scattering along the x -axis. We call such an effect the plasmonic transverse phase resonances, which can give rise to rich features of the transmission spectrum, such as sharp dips [26,27]. Using these phase information along the x -direction, we can see the relationship between the resonant frequency and the number of anti-phase (π phase) change on the adjacent grooves (a typical hybridization effect). For the resonance at ω_2 , the field at every narrow groove is in anti-phase with its nearest neighbor, which results in a relatively high resonant frequency; this is consistent with our finding that $\omega_2 > \omega_1$ because only groove #1 is in anti-phase with its neighbors at ω_1 .

For the two resonances of the second type (ω_3 and ω_4) generated due to mode splitting on the basis of the second order of the original T-groove resonance (ω_{b2}), they are also quite different from each other in terms of the phase information around the input opening of the narrow grooves along x -direction. In detail, the phase distribution at ω_3 and ω_4 can be represented by ‘+ + + +’ and ‘- - - -’, respectively. Besides, we find that $\omega_3 < \omega_4$, that is because there is no anti-phase adjacent groove at ω_3 , while groove #3 is in anti-phase with its neighbors at ω_4 .

From a different point of view, we could also regard our proposal as a double-layer structure comprising of the top nanostrip layer and the bottom nanogroove layer. Our study shows that our double-layer metallic surface works much better in comparison with the case of a single layer with only the narrow grooves which displays only one weak absorption peak ($\eta_{max} = 38\%$) at $\hbar\omega = 0.55$ eV at normal incidence as shown in Fig. 2(a) by the cross line. This also means that nearly three-fold of improvement of absorption is achieved after adding the top nanostrip layer, in conjunction of additional peaks due to mode splitting.

An important practical issue for such a double-layer structure is that, careful alignment between layers in the fabrication process may be necessary. Therefore, we study the absorption dependence on such alignment error. We define a parameter S_x as the distance between the center of the top wide air gap and the center of the bottom narrow groove (#3) along the x -axis. We tune S_x from 0 to $P/8$ (only this range is considered because all the bottom narrow grooves are identical) and plot the absorption spectra at normal incidence in Fig. 4(a). Apparently, when S_x lies in the range between 0 to 100 nm and the absorption efficiency of our system within the considered frequency range is almost invariant. When $S_x > 100$ nm (i.e., the center of top wide air gap is far from the center of bottom narrow groove), the resonance at ω_2 becomes weaker and finally disappears, while other three

absorption peaks are not influenced at all. In this sense, our light absorber is quite robust and fairly insensitive to alignment error.

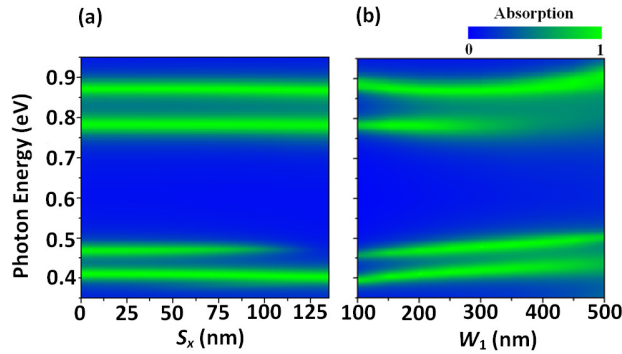


Fig. 4. Absorption spectra at normal incidence when the relative position of different layers along x direction (S_x) is tuned (a) and when the width of top wide air gap (W_1) is tuned (b).

In Fig. 4(b), we also plot the absorption at normal incidence as the width of the top wide air gap (W_1) varies in the range of 100 to 500 nm. One sees that the resonances at ω_1 and ω_2 have only a slight blueshift when W_1 increases. But the resonances at ω_3 and ω_4 have a very small redshift when W_1 is smaller than 300 nm because the mode volume is increased in-between neighboring nanostrips and then a slight blueshift when W_1 is larger than 300 nm because the resonant mode under the nanostrip has been compressed. Figure 4(b) also shows that the absorption efficiency for the resonance at ω_3 becomes much weaker when W_1 is larger than 300 nm because its excitation condition has been destroyed gradually. Additionally, it is indicated that the spectrum is almost insensitive to the width of the top wide air gap within the range from $W_1 = 100$ nm to 300 nm.

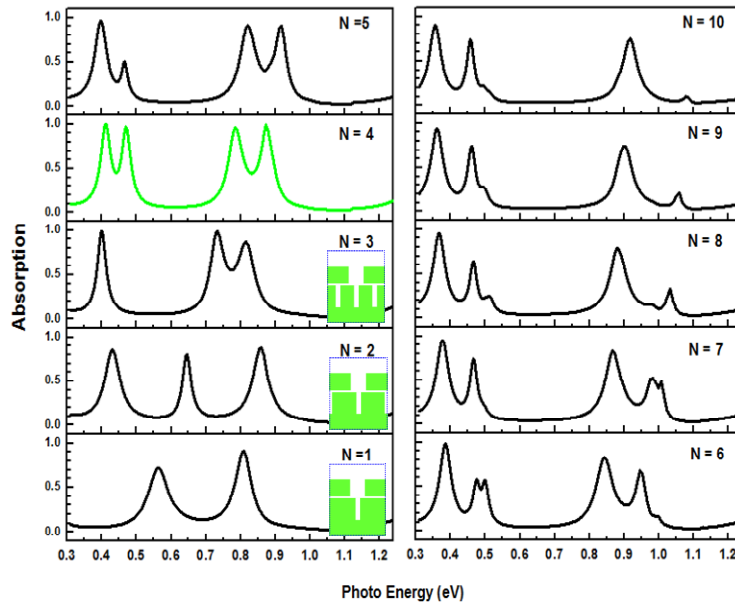


Fig. 5. Absorption spectra at normal incidence when the number of narrow grooves (N) in each period varies. 2-D configurations for the cases of $N = 1$ to 3 are shown in the insets.

Our study also indicates that there is an optimal absorption enhancement with respect to the number of the narrow grooves in each period, as shown in Fig. 5. When the grooves are

added gradually from 1 to 3, the number of the absorption peaks increases due to mode splitting. When N equals to 4, the above-mentioned four phase states are all perfectly excited. However, further increase of groove number N does not improve absorption effectively. For example, when $N = 8$, we can obtain more than three sub-bands near 0.4 eV. But the efficiency for some bands is pretty low because of phase mismatch.

4. Conclusions

In conclusion, we have demonstrated an efficient light absorber by a novel hybrid grating structure inspired by V-groove metallic surfaces. By introducing a small horizontal gap and additional narrow grooves which support additional transverse phase resonances, the overall metallic surface displays four strong absorption peaks at infrared frequencies. For the origin of the peaks, we need to emphasize that both of the additional narrow grooves and the horizontal gap are very important. The additional narrow grooves are responsible to generate lattice scattering along the x -axis to cause the transverse phase resonances. The horizontal gap plays the role to make such lattice scattering effect possible by feeding energy into the narrow grooves. Our study has shown that the present structure is robust and does not require highly accurate alignment in fabrication. We have also shown that some of the generated absorption peaks exhibit wide-angle characteristic.

Acknowledgments

This work is partially supported by the National Science Foundation (CMMI 0846771), the National Natural Science Foundation of China (60990320 and 60901039), and AOARD (114045). Cui acknowledges Natural Foundation of Shanxi (2012011020-4), Special Foundation of Taiyuan University of Technology (No. 2012L033), and the Starting Research Fund from Taiyuan University of Technology.